Digital Track Following Control of Hard Disk Drives with Dual Stage Actuation —- Multi-rate Control Implementation for Computation Saving

Jiagen Ding, Federico Marcassa, and Masayoshi Tomizuka
Department of Mechanical Engineering
University of California at Berkeley, Berkeley, CA 94720-1740
jgding@newton.Berkeley.edu, marcassa@dei.unipd.it and tomizuka@me.Berkeley.edu

Abstract

This report is concerned with digital track following control of hard disk drives with dual stage actuation. The dual stage actuator considered in this study consists of a voice coil motor (VCM) as the first stage actuator and a piezoelectric transducer (PZT) as the second stage actuator. The second stage actuator is introduced to enlarge the control bandwidth. The number of sectors for embedded servo must be determined so that the sampling rate of the position error signal is consistent with the desired servo bandwidth. Such a sampling rate is applied to the PZT servo loop, but the VCM servo loop does not have to be closed at the same rate. Namely, the VCM servo loop may be closed at a slower rate to reduce the total amount of computation without a significant deterioration of track following performance. Such multi-rate implementations of digital control algorithms are considered. Analysis is based on lifting. The effectiveness of the proposed multi-rate implementation schemes is demonstrated by simulations and experiments.

Multi-rate Digital Control, Computation Saving, Lifting , Performance Analysis, Dual Actuator and Hard Disk Drives

1 Introduction

A practical multi-rate controller design deals with the following problem: the plant output is sampled at a limited frequency and the controlling input is updated at a faster frequency to achieve better performance. One classic example is the single actuator disk file system, where the position error signal(PES) sampling frequency is limited by the number of sectors and the rotating speed[1]. Another practical case is a plant consisting of multiple actuators with different bandwidths. In this case, it may make sense that the control inputs are updated at slow sampling rates for low bandwidth actuators and at fast sampling rates for the high bandwidth actuators. Finally, multi-rate control can be used when the control algorithm in a single loop controller can be separated into fast modes and slow modes [9]. In this case, it is natural to update the slow mode controller at a slow sampling frequency and the fast mode controller at a fast sampling frequency. The multi-rate design goal here is to achieve a low cost solution via computation saving. A multi-actuator example is the dual actuator disk file system where the plant consists of two actuators: coarse and fine actuators. The coarse actuator is low bandwidth but has a large stroke; the voice coil motor (VCM) is the most popular coarse actuator. The fine actuator is high bandwidth but has a small stroke; The piezoelectric transducer(PZT) is a popular fine actuator[4]. One example for the controller mode separation is the single actuator disk file system where the digital controller consists of digital integrator and lead-lag phase compensator. The slow mode controller corresponds to the digital integrator and the fast mode corresponds to the digital phase compensator.

Multi-rate design and analysis have been widely studied for achieving better performance[1],[2]. In [2], the plant output is sampled at a limited frequency and the multi-rate design is to design a state estimator working at a fast sampling frequency after the original plant output is interpolated by repetition. In [3], the multi-rate design is similar to [2] and the output sensitivity function is computed for evaluating disturbance rejection. In [5], the lifting technique is used to reduce the multi-rate discrete-time problem to a norm-equivalent discrete-time

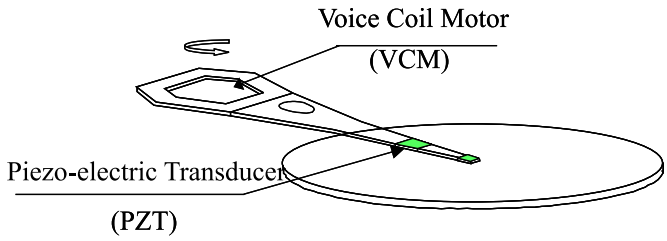

Figure 1: Dual Actuator Servosystem

problem, to which standard methods can be applied. More lifting based multirate control can be found in[10] and [11]. In [8], a multi-rate design method for computation saving is proposed by approximating the slow sampling frequency path at a fast sampling frequency. This report will explore the multi-rate scheme from the view point of computation saving.

The remainder of this report is organized as follows. Section 2 presents two cases of multirate control for computational saving. Section 3 analyzes the multirate system via the lifting technique. Section 4 presents the performance analysis for disturbance rejection in the multi-rate system. Section 5 demonstrates an application example, dual actuator track following control of a hard disk drive with experimental results. Concluding remarks are given in section 6.

2 Multirate Control for Computational Saving

In this section, two cases of multirate control for computational saving are presented. The two cases are presented for control of the recording head of hard disk drives(HDD), but similiar cases may be easily found in other motion control problems.

Magnetic hard disk drive storage technology continues to experience a dramatic areal density growth of 60% every year [13] and the future density will reach levels as high as $100Gb/in^2$. Very narrow data tracks are required in order to obtain such high densities. High bandwidth servo is necessary for track following with such a narrow track pitch. Dual actuator servo(Fig.1) is one way to enlarge the servo bandwidth. Dual actuator disk servo consists of two actuators: a coarse and a fine actuator. The coarse actuator is low bandwidth

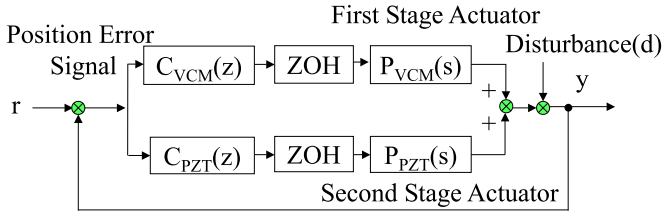

Figure 2: Block Diagram of Dual Actuator Servo System for Hard Disk Drive

with a large stroke, and the voice coil motor (VCM) is the most popular coarse actuator; the fine actuator is high bandwidth with a small stroke, and the piezoelectric transducer(PZT) is a popular fine actuator.

The dynamics of the VCM and PZT are represented by $P_{VCM}(s)$ and $P_{PZT}(s)$, respectively. The control block diagram for the dual actuator servosystem becomes as depicted in Fig.2. In the figure, the digital controller for VCM and that for PZT are represented by $C_{VCM}(z)$ and $C_{PZT}(z)$, respectively. Note that the input to $C_{VCM}(z)$ and $C_{PZT}(z)$ are both the position error signal. In view of the high bandwidth nature of PZT, a logical question is whether the PZT controller and VCM controller need to be updated at the same frequency. As will be revisited by experiments in the later section, there is no significant degradation of performance if the VCM controller is updated at a frequency lower than the PZT controller. If the VCM controller is updated at a slow rate, the block diagram of Fig. 2 is modified to the one in Fig. 3. In the figure, D and I represent decimation and interpolation respectively, and m denotes the multirate ratio. The decimator picks up the position error signal at every m instances of the fast sampling frequency $f_f(=\frac{1}{T_f})$, and the VCM controller is updated at the slow rate $f_f/m(=\frac{1}{T_s})$. The interpolator converts the VCM output defined at the slow rate to the fast rate by repetition. $C_{VCM}(z^m)$ must be obtained so that its input output characteristics remains close to that of $C_{VCM}(z)$. One method to achieve this is summarized below.

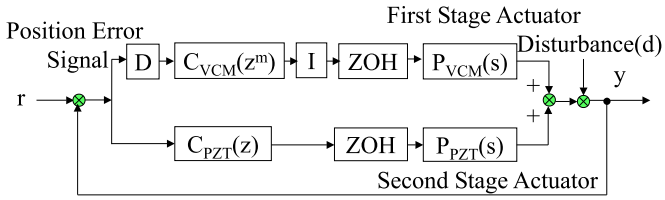

Figure 3: Multirate Implementation of Dual Actuator Servosystem

Step 1. Obtain a state space realization of $C_{VCM}(z)$. Denote it as:

$$\begin{aligned} x_c(k+1) &= A_c x_c(k) + B_c e(k) \\ u_{vcm}(k) &= C_c x_c(k) + D_c e(k) \end{aligned} \tag{1}$$

where $e(k)$ and $u_{vcm}(k)$ are the position error signal and the output of the VCM controller at the k-th fast sampling instance. Notice that $C_{VCM}(z)$ and Eq.2 are related by:

$$C_{VCM}(z) = C_c(zI - A_c)^{-1}B_c + D_c \tag{2}$$

Obviously, the choice of $\{A_c, B_c, C_c$ and $D_c\}$ is not unique given $C_{VCM}(z)$.

Step 2. Assume that the input to $C_{VCM}(z)$ does not change from the fast sampling instance mk to $mk+m-1$. Then, from Eq. 2,

$$\begin{aligned} x_c(m(k+1)) &= A_c^m x_c(mk) + \sum_{j=0}^{m-1} A_c^{m-1-j} B_c e(mk+j) \\ &= A_c^m x_c(mk) + (\sum_{j=0}^{m-1} A_c^{m-1-j} B_c) e(mk) \\ u_c(mk) &= C_c x_c(mk) + D_c e(mk) \end{aligned} \tag{3}$$

Step 3. Applying z-transformation to Eq. 3:

$$C_{VCM}(z^m) = C_c(z^m I - A_c^m)^{-1}(\sum_{j=0}^{m-1} A_c^{m-1-j} B_c) + D_c \tag{4}$$

Remark 1. Notice from Eqs.2 and 4 that the order of the VCM controller remains the same whether it is updated at a fast rate or a slow rate. This implies that the total amount

of computation is on average significantly reduced by implementing the VCM controller at a slow rate. The computation saving, however, is not uniform over m consecutive fast sampling instances: at $k = mj(j = 0, 1, 2, ...)$, the amount of computation to implement Eq. 4 is as much as that to implement Eq. 2, and at other time instances $k \neq mj$, no computation is performed. This nonuniform nature may be overcome by introducing the idea of interlacing, which will be stated after Remark 2 below.

Remark 2. If the original controller is expanded by partial fraction expansion, i.e.

$$C_{VCM}(z) = C_{VCM1}(z) + C_{VCM2}(z) + ... + C_{VCMl}(z) \tag{5}$$

it is possible to apply the three step procedure above to each block in the right hand side of Eq .5. Furthermore, it is also possible to apply different update rates to each block. For example, implement the first two blocks at a fast rate and the remaining block at a slow rate with a multirate ratio of m. In this case, the three step procedure is applied only to the blocks implemented at the slow rate.

2.1 Multirate Control with Interlacing

Assume that the multirate ratio m is selected so that the VCM controller $C_{VCM}(z)$ may be naturally decomposed to m blocks: i.e.

$$C_{VCM}(z) = C_{VCM1}(z) + C_{VCM2}(z) + ... + C_{VCMm}(z) \tag{6}$$

where $n_c = n_{c1} + n_{c2} + ... + n_{cm}$, n_c is the order of $C_{VCM}(z)$ and n_{ci} is the order of $C_{VCMi}(z)$(i=1,2, ...,m). Obviously

$$n_{max} = \max_i(n_{ci}) < n_c \tag{7}$$

Applying the three step procedure, the controller for the slow sampling rate is

$$C_{VCM}(z^m) = C_{VCM1}(z^m) + C_{VCM2}(z^m) + ... + C_{VCMm}(z^m) \tag{8}$$

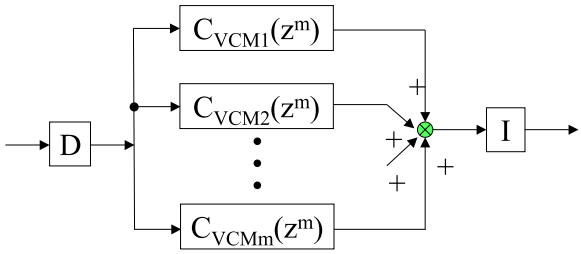

Figure 4: Slow rate Implementation of $C_{VCM}(z)$

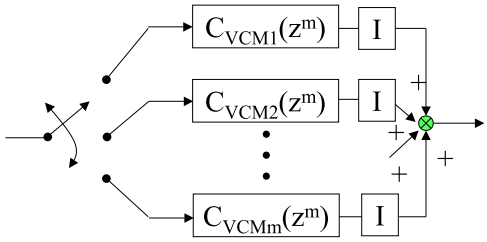

Figure 5: Slow rate Implementation of $C_{VCM}(z)$ with Interlacing

This controller can be implemented as illustrated in Fig. 4. Instead of updating $C_{VCMi}(z^m)$(i=1,2,..,m) all at the same sampling instances, $C_{VCMi}(z^m)$ may be updated one block at a time at fast sampling instances: i.e. update C_{VCMi} at $k = mj + i - 1(j = 0, 1, 2, ...)$. This is an interlacing operation, and the controller implementation diagram becomes as shown in Fig. 5. In this implementation, the amount of computation required at each fast sampling instance is equivalent to or less than that of implementing an n_{max}-th order digital controller, and compuation saving is more uniform by distributing computation among each fast sampling point.

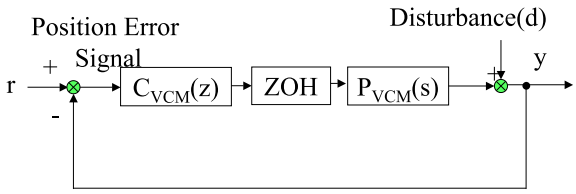

Figure 6: VCM Driven HDD Servosystem

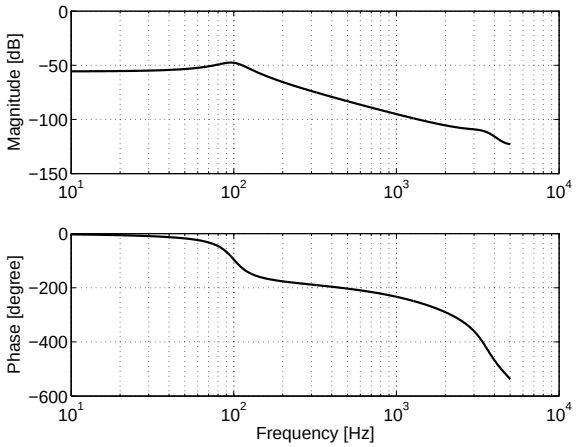

Figure 7: Frequency Response of VCM

2.2 Decomposition of Controller to Fast-mode and Slow-mode Components [8]

Dynamic controllers normally have slow dynamics and fast dynamics. For example, in PID(Proportional plus Integral plus Derivative) Control, I-action represents slow dynamics and D-action represents fast dynamics. As an example, consider a VCM-driven HDD servo system depicted in Fig. 6. The controlled plant $P_{VCM}(s)$ (a suspension carriage assembly driven by VCM) is characterized by the the frequency response is Fig. 7. For a sampling period of $99\mu s$, one digital controller to achieve design objectives is :

$$C_{VCM}(z) = 7.5e4 \frac{(z-0.9971)(z-0.9387)^2}{(z-0.9999)(z-0.9987)(z+0.2142)} \tag{9}$$

Notice that this controller can be expanded as:

$$\begin{aligned} C_{VCM}(z) &= C_{VCM1}(z) + C_{VCM2}(z) + C_{VCM3}(z) + K_D & (10) \\ &= \frac{5.19e2}{z-0.9999} + \frac{-2.75e2}{z-0.9987} + \frac{-8.20e4}{z+0.2142} + 7.5e4 & (11) \end{aligned}$$

In this expansion, the first two blocks represent slow dynamics and it is expected that they can be updated every other sampling instances without a significant performance degradation. Then, a multirate implementation of the controller with interlacing becomes as depicted in Fig.8. Notice that the multirate ratio in this implementation is 2. Since each of $C_{VCMi}(i =$

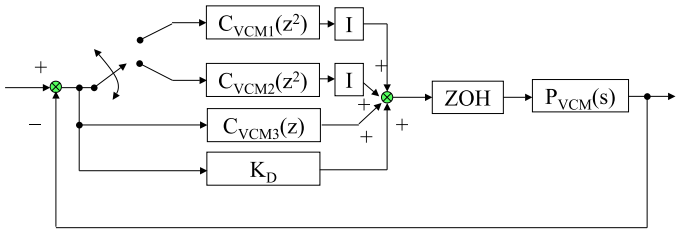

Figure 8: Multirate Implementation of Digital Controller

$1, 2, 3$) is a first order block, two first order blocks are updated at every sampling instance. If the controller is implemented at a single rate, three first order blocks must be updated at each sampling instance. This implies that the multi-rate implementation saves computation by about 33%. See Wu and Tomizuka[9] for further aspects of multirate implementation of digital controllers after decomposition to fast-mode and slow-mode components. In [9], a guideline for classifying dynamic modes to slow and fast components is given.

3 Analysis of Multi-rate Systems via Lifting

An important performance measure of feedback control system is rejection characteristics of disturbances, i.e. sensitivity. A convenient method for sensitivity analysis of multirate systems is based on lifting[5]. Lifting converts the multi-rate system to an equivalent single rate system, the sampling frequency of which is the slow rate. In this section, lifting of various subsystems in multi-rate systems for computation saving is presented.

3.1 Lifting of the Controlled Plant(Actuator)

Consider a plant(actuator) where the input and the output are related by the following equation:

$$y(k) = P(z)u(k) \tag{12}$$

where z is one-step advance operator corresponding to a fast sampling frequency $\frac{1}{T_f}$. Assume that the multi-rate ratio is m. Then, the lifted input $U(k)$ and output $Y(k)$ at the slow rate are:

$$U(k) = \begin{bmatrix} u(mk) \\ u(mk+1) \\ . \\ . \\ . \\ u(mk+m-1) \end{bmatrix} \tag{13}$$

$$Y(k) = \begin{bmatrix} y(mk) \\ y(mk+1) \\ . \\ . \\ . \\ y(mk+m-1) \end{bmatrix} \tag{14}$$

Notice that the H_2 norm of a signal remains unchanged after lifting. Let state space representation of P(z) be:

$$x(k+1) = Ax(k) + Bu(k) \tag{15}$$

$$y(k) = Cx(k) + Du(k) \tag{16}$$

Then, the lifted input and output vectors, $U(k)$ and $Y(k)$, are related by the transfer function maxtrix[6].

$$P_L(z^m) = \begin{bmatrix} C \\ CA \\ . \\ . \\ . \\ CA^{m-1} \end{bmatrix} (z^m I - A^m)^{-1} [A^{m-1}B \; A^{m-2}B \; \ldots \; AB \; B] \tag{17}$$

$$+ \begin{bmatrix} D & 0 & 0 & . & . & . \\ CB & D & 0 & . & . & . \\ CAB & CB & D & . & . & . \\ . & & & & & \\ . & & & & & \\ . & & & & & \\ CA^{m-2}B & CA^{m-3}B & . & . & . & D \end{bmatrix}$$

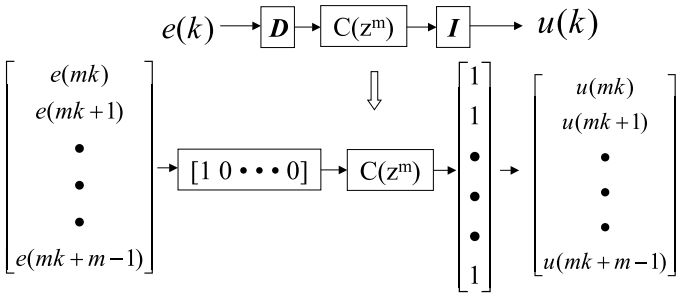

Figure 9: Lifting of Slow-Rate Block

3.2 Lifting of Controllers

3.2.1 Lifting slow rate block (no interlacing)

Figure 9 shows the lifting of slow rate block which does not involve interlacing. The error signal is decimated before being fed to the controller $C(z^m)$ and the slow rate control input $u(k)$ interpolated by repetition. The lifted control input $U(k)$ is related to the lifted error signal $E(k)$ by:

$$U(k) = \begin{bmatrix} 1 \\ 1 \\ . \\ . \\ . \\ 1 \end{bmatrix} C(z^m) \begin{bmatrix} 1 & 0 & . & . & . & 0 \end{bmatrix} E(k) \tag{18}$$

where $E(k)$ is given as:

$$E(k) = \begin{bmatrix} e(mk) \\ e(mk+1) \\ . \\ . \\ . \\ e(mk+m-1) \end{bmatrix} \tag{19}$$

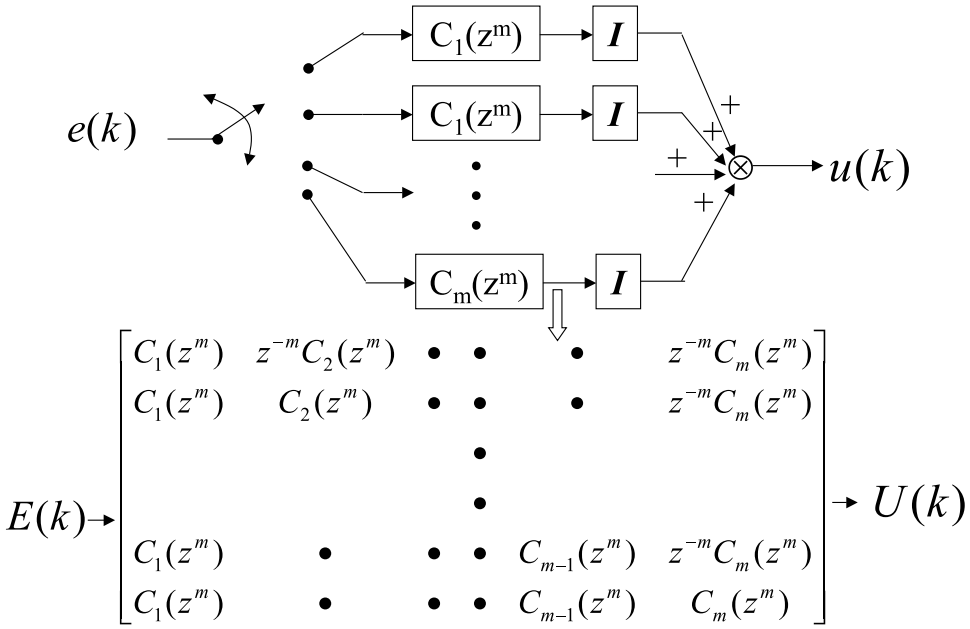

Figure 10: Lifting Interlacing Block

3.2.2 Lifting slow rate block (interlacing)

Figure 10 shows the lifting of slow rate block which involves interlacing. The lifted control input $U(k)$ is related to the lifted error signal $E(k)$ by:

$$U(k) = \begin{bmatrix} C_1(z^m) & z^{-m}C_2(z^m) & . & . & . & z^{-m}C_m(z^m) \\ C_1(z^m) & C_2(z^m) & z^{-m}C_3(z^m) & . & . & z^{-m}C(z^m) \\ . & & & & & \\ . & & & & & \\ . & & & & & \\ C_1(z^m) & C_2(z^m) & . & . & . & C_m(z^m) \end{bmatrix} E(k) \qquad (20)$$

3.2.3 Lifting fast rate block

The relation between lifted input signal $E(k)$ and $U(k)$ for the fast rate block (Fig. 11) can be obtained by following the procedure explained for the plant dynamics in III A. For this purpose, the controller $C(z)$ must be expressed in the state space form $\{A_c, B_c, C_c, D_c\}$. Alternatively, $C(z)$ may be expressed in the impulse response form and decomposed as follows.

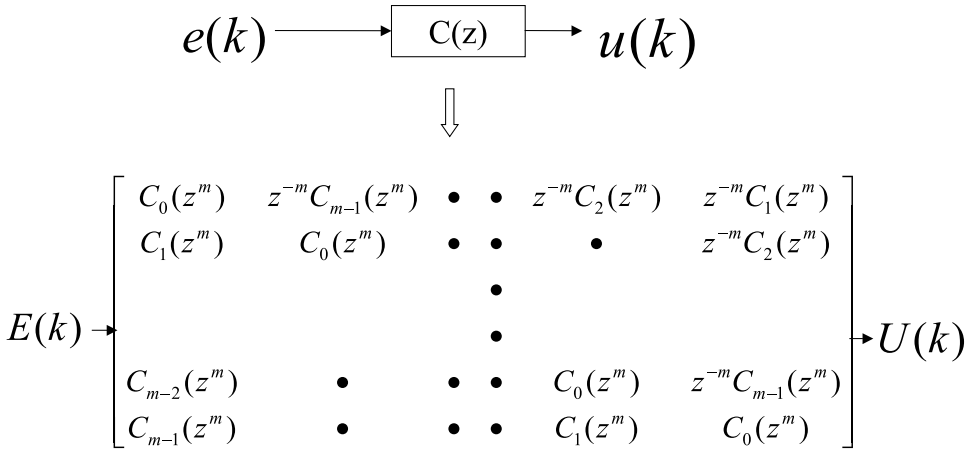

Figure 11: Lifting Fast Rate Block

$$
\begin{aligned}
u(mk) &= C(z)e(mk) \qquad (21)\\
&= (\sum_{j=0}^{\infty} c(j)z^{-j})e(mk)\\
&= [\sum_{l=0}^{\infty} c(ml)z^{-ml} + \sum_{l=0}^{\infty} c(ml+1)z^{-(ml+1)} + ... + \sum_{l=0}^{\infty} c(ml+m-1)z^{-(ml+m-1)}]e(mk)\\
&= [\sum_{l=0}^{m-1} c_i(z^m)z^{-i}]e(mk)\\
&= C_0(z^m)e(mk) + z^{-m}C_1(z^m)e(mk+m-1) + ...\\
&\quad +z^{-m}C_{m-1}e(mk+m-(m-1))
\end{aligned}
$$

Thus, the lifted input and output are related by:

$$
U(k) = \begin{bmatrix}
C_0(z^m) & z^{-m}C_{m-1}(z^m) & . & . & . & z^{-m}C_1(z^m)\\
C_1(z^m) & C_0(z^m) & z^{-m}C_{m-1}(z^m) & . & . & z^{-m}C_2(z^m)\\
. & & & & & \\
. & & & & & \\
. & & & & & \\
C_{m-1}(z^m) & . & . & . & C_1(z^m) & C_0(z^m)
\end{bmatrix} E(k) \qquad (22)
$$

3.3 Overall System in Lifted Space

A general multirate control system is an interconnected control blocks and plants(actuators). The control blocks may be implemented in fast sampling rate, slow sampling rate without interlacing or slow sampling rate with interlacing and the plants(actuators) are operating at fast sampling rate. The lifting can be applied to this general multirate control system as follows. First, the plants are lifted to slow rate system and the corresponding transfer matrices are given by applying Eq. 17. Second, the slow rate control blocks without interlacing and with interlacing can be lifted to slow rate control blocks using Eq. 18 and 20, respectively. Next, the fast rate control blocks are converted to slow rate control blocks via lifting by applying Eq. 17 for $\{A_c, B_c, C_c, D_c\}$ or Eq. 22. Finally, the lifted plants and control blocks can be combined into one transfer matrix via the interconnection. Figure 12 shows such an example: i.e. the lifted dual actuator HDD block diagram with multi-ratio 2. $C_{VCML}(z^2)$, $C_{PZTL}(z^2)$, $P_{VCML}(z^2)$ and $P_{PZTL}(z^2)$ denotes the lifted VCM slow rate controller, the lifted PZT high rate controller, the lifted high rate VCM and PZT plants, respectively. Figure 13 shows a lifted system with multi-ratio 2 by combining all the controllers and plants into a transfer matrix M.

The stablility and performance of the original multirate system can be analyzed through its lifted single slow rate system. Notice that lifting is 2-norm invariant transformation and the stability of the original multirate system can be checked by examing the stability of the single slow rate lifted system. Details about the stability analysis for multivariable system can be found in [15].

Remark 3. Recall that in our proposed multirate control, the slow and fast rate implementation of the controllers have similiar input and output transfer characteristics. Thus, the slow rate implementation of controllers will less likely cause stability problems.

The sensitivity based performance analysis for multirate system is discussed in the next section via lifting.

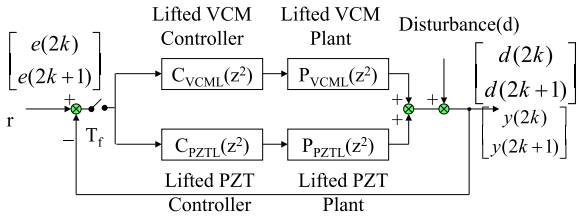

Figure 12: Lifted System with Two Different Bandwidth Actuators

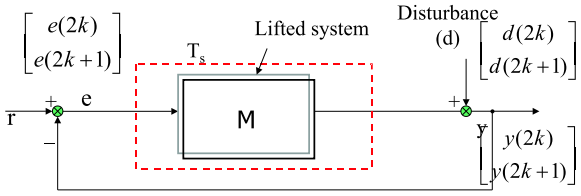

Figure 13: Lifted System for Disturbance Rejection

4 Performance Indices for Multi-rate Systems

Referring to Fig. 13, the disturbance rejection transfer matrix S_L for the lifted disturbance signal is:

$$S_L(z^2) = (I + M(z^2))^{-1} \tag{23}$$

If we apply a standard method from the multivariable control theory, the performance index for disturbance rejection is:

$$Index_1 = \overline{\sigma}[(I + M(e^{j\omega T_s})^{-1}] \tag{24}$$

where $\overline{\sigma}$ denotes the maximum singular value and we have noted $z = e^{T_f s}$ and $T_s = 2T_f$.

We recall that the maximum singular value is nothing but the induced l_2 norm of the matrix. Namely, $Index_1$ gives the maximum amplification factor from the lifted disturbance vector to the lifted output vector but it ingores the relation between the first and second components of the lifted disturbance vector, a consequence of which is an unrealistic prediction of disturbance rejection, in particular, at low frequencies. If we are evaluating the frequency response from the disturbance $d(k)$ to the output $y(k)$, the disturbance at the even

time instances $d(2k)$ and the odd time instances $d(2k+1)$ are related to each other and may be written in the complex form

$$d(2k) = e^{j\omega T_f 2k} \; and \; d(2k+1) = e^{j\omega T_f (2k+1)} \tag{25}$$

Then, the lifted disturbance vector is

$$D(2k) = \begin{bmatrix} d(2k) \\ d(2k+1) \end{bmatrix} = \begin{bmatrix} 1 \\ e^{j\omega T_f} \end{bmatrix} e^{j\omega T_f 2k} = \begin{bmatrix} 1 \\ e^{j\frac{\omega T_s}{2}} \end{bmatrix} e^{j\omega T_s k} \tag{26}$$

By introducing a scaling factor so that $||D(2k)||_2 = 1$, The amplification of the disturbance on the output may be judged for each frequency $\omega_s (\frac{-\pi}{T_s} \leq \omega_s \leq \frac{\pi}{T_s})$ by

$$Index_2 = \overline{\sigma}[(I + M(e^{j\omega T_s}) \begin{bmatrix} 1/\sqrt{2} \\ e^{j\omega T_s/2}/\sqrt{2} \end{bmatrix}] \tag{27}$$

For multi-ratio m, $Index_2$ becomes

$$Index_2 = \overline{\sigma}[(I + M(e^{j\omega T_s}) \begin{bmatrix} 1/\sqrt{m} \\ e^{j\omega T_s/m}/\sqrt{m} \\ \cdot \\ \cdot \\ \cdot \\ e^{j(m-1)\omega T_s/m}/\sqrt{m} \end{bmatrix}] \tag{28}$$

At low frequencies, good approximation of Eq.26 is

$$D(2k) = \begin{bmatrix} d(2k) \\ d(2k+1) \end{bmatrix} = \begin{bmatrix} 1 \\ e^{j\omega T_f} \end{bmatrix} e^{j\omega T_f 2k} \approx \begin{bmatrix} 1 \\ 1 \end{bmatrix} e^{j\omega T_s k} \tag{29}$$

Thus, we have

$$Index_3 = \overline{\sigma}[(I + M(e^{j\omega T_s}) \begin{bmatrix} 1/\sqrt{2} \\ 1/\sqrt{2} \end{bmatrix}] \tag{30}$$

for multi-ratio 2 and

$$Index_3 = \overline{\sigma}[(I + M(e^{j\omega T_s}) \begin{bmatrix} 1/\sqrt{m} \\ 1/\sqrt{m} \\ \cdot \\ \cdot \\ \cdot \\ 1/\sqrt{m} \end{bmatrix}] \tag{31}$$

for multi-ratio m. As will be numerically shown in the next section, $Index_2$ and $Index_3$ give realistic predictions of disturbance rejection by multi-rate control.

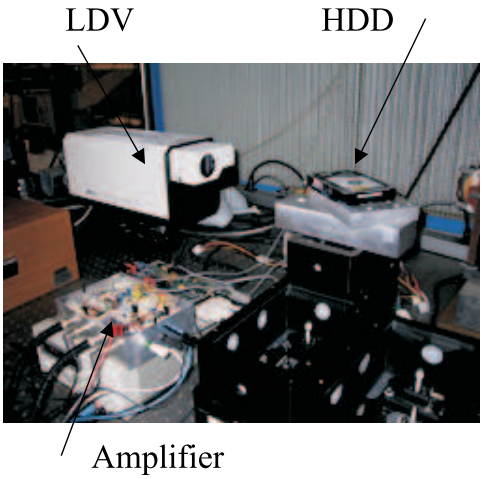

Figure 14: Dual Actuator Setup

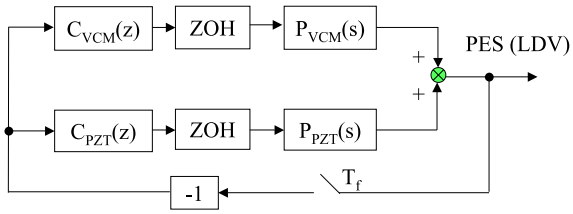

Figure 15: Parallel Track Following Diagram

5 Application Example in Dual Actuator Track Following

The experimental setup for dual actuator disk drives is depicted in Fig. 14. It includes a conventional actuator voice coil motor, a Hutchinson PZT based micro-actuator, a digital signal processor(TI TMS230C67X DSP), and a laser doppler vibrometer(LDV) for measuring the position error. All the digital controllers are implemented on the DSP. The fast sampling rate is $\frac{1}{T_f}(50kHz)$ and the slow sampling rate is $\frac{1}{3T_f}$: i.e. the multi-ratio is 3

Figure 15 shows the single fast rate parallel dual actuator track following system. P_{VCM} and P_{PZT} denote the VCM and PZT plant, respectively. Figures 17 and 18 shows the frequency response of the VCM and the PZT, respectively. C_{VCM} and C_{PZT} denote the VCM and PZT controller respectively. They are given as:

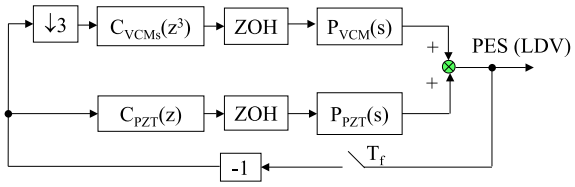

Figure 16: Multi-rate Implementation of Digital Controller for Track Following

$$C_{VCM}(z) = 4.0681\frac{(z-0.9905)(z-0.9756)(z-0.9057)}{(z-1)(z-0.9577)(z-0.8664)} \tag{32}$$

$$C_{PZT}(z) = 4.2646\frac{(z-0.9996)(z-0.5042)}{(z-0.9991)(z-0.9681)} \times\frac{(z^2-1.148z+0.9983)(z^2-1.518z+0.9817)}{(z^2-0.9841z+0.5536)(z^2-1.343z+0.7729)} \tag{33}$$

Figure 19 shows the total open loop frequency response.

Figure 16 shows the multi-rate dual actuator track following system with multi-rate ratio 3. denotes the VCM controller working at slow rate and its transfer function is obtained as:

$$C_{VCMs}(z^3) = 3.8948\frac{(z^3-0.9719)(z^3-0.9285)(z^3-0.7414)}{(z^3-1)(z^3-0.8726)(z^3-0.6465)} \tag{34}$$

Figure 20 shows the implementation of the interlaced VCM controller at slow rate. Notice that the slow rate VCM controller is divided into 3 parallel sub-controllers:

$$\begin{aligned} C_{VCM1}(z^3) &= \frac{0.04498}{z^3-1} \\ C_{VCM2}(z^3) &= \frac{-0.09843}{z^3-0.8726} \\ C_{VCM3}(z^3) &= \frac{3.895z^3-2.942}{z^3-0.6465} \end{aligned} \tag{35}$$

A constant term appearing in the expansion of Eq. 34 has been absorbed in C_{VCM3}.

Figures 21 and 23 show the performance indices for multi-rate system without interlacing and multi-rate with interlacing. Zoom in of the performance indices at high frequencies(around 8kHz) is shown in Figs. 22 and 24. Notice that $Index_1$ suggests that disturbance

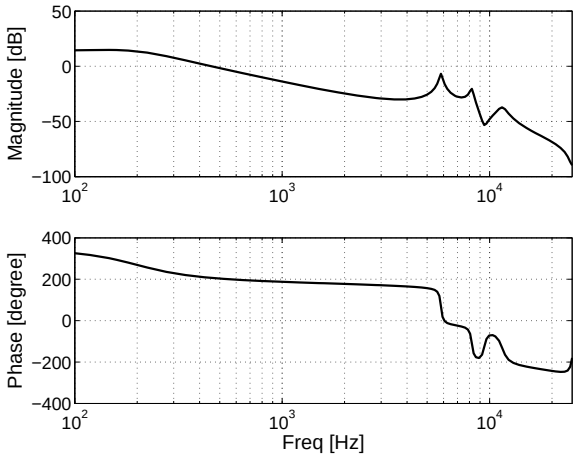

Figure 17: VCM Plant

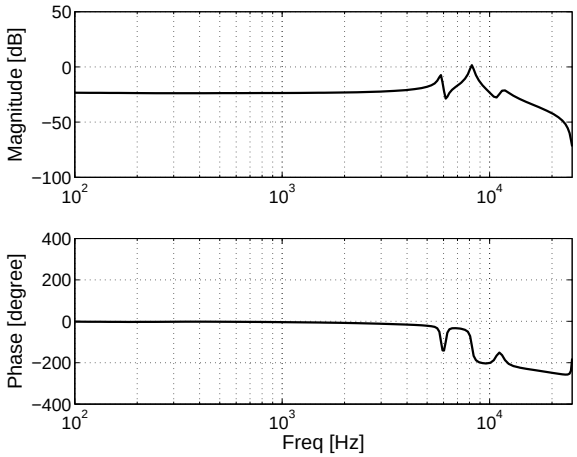

Figure 18: PZT Plant

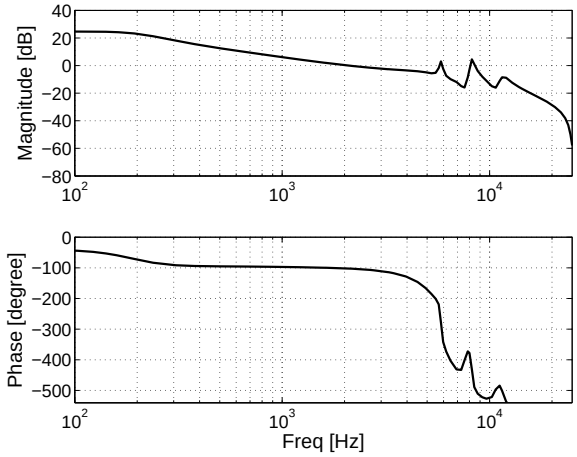

Figure 19: Total Open Loop Frequency Response at Single Fast Rate

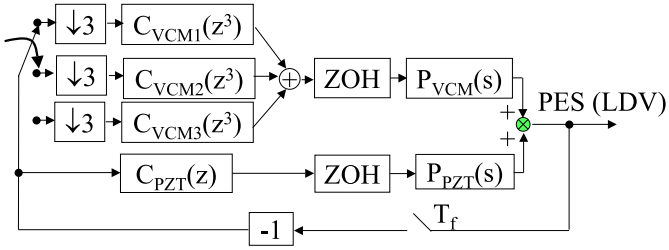

Figure 20: Multi-rate Implementation of Digital Controller with Interlacing for Track Following

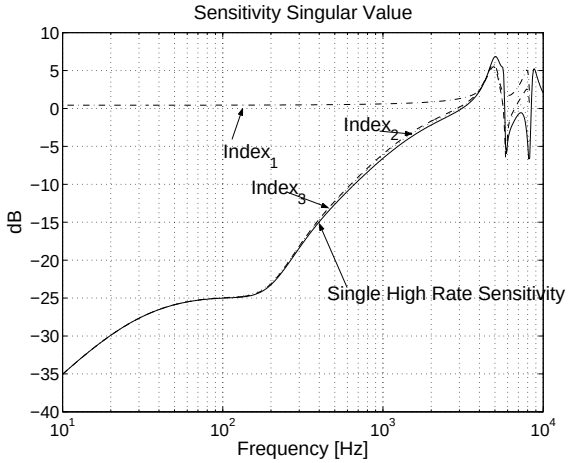

Figure 21: Index Computation for Multi-rate Implementation without Interlacing

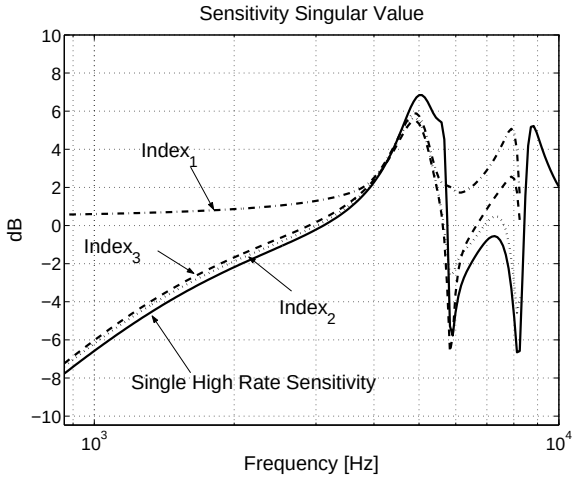

Figure 22: Zoom In of Index Computation for Multi-rate Implementation without Interlacing

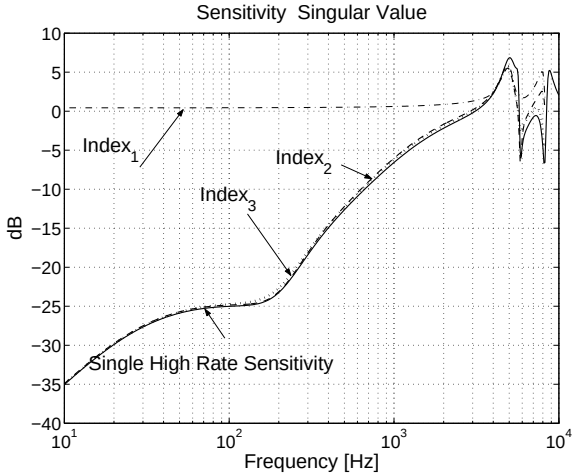

Figure 23: Index computation for Multi-rate Implementation with Interlacing

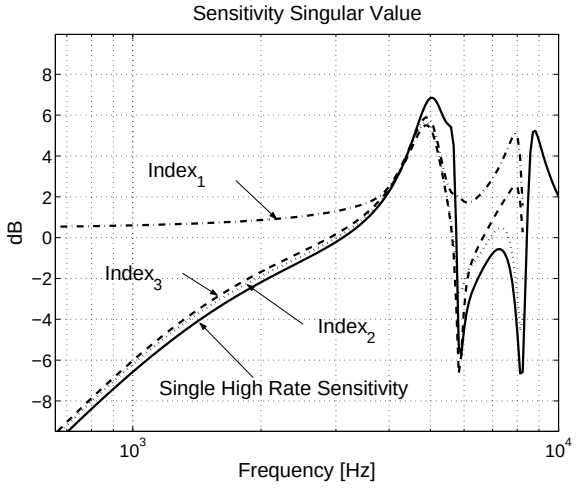

Figure 24: Zoom In of Index computation for Multi-rate Implementation with Interlacing

rejection does not take place at low frequencies, and that $Index_2$ is very close to the single fast rate sensitivity function. $Index_3$ approximates $Index_2$ well at low frequencies. As shown later, experimental results indicate that the performance of fast single rate implementation and that of multi-rate implementation are close to each other. This confirms that $Index_2$ and $Index_3$ are realistic measures of disturbance rejection while $Index_1$ is too conservative. They also indicate that the performance degradation due to slow rate implementation is primarily at high frequencies but is minimal in this example.

The controller was implemented in assembly language. The TI DSP operates at at $150MHz$ and it includes two sets of register banks, the floating point unit(MAC) and several integer functional units(Adder,Multiplier). The codes for the digital controller are optimized to achieve the least computing cycles. Table 1 summarizes the number of assembly instructions used in the fast rate PZT controller over T_f. To execute these instructions, 159 cycles are needed over $T_s = 3T_f$. Table 2 summarizes the numbers of assembly instructions for

Table 1: Number of Instructions in PZT Controller

Instructions	fast rate
Move	36
Mult/Add/Floating	27
Nop	22
Branch	0

the VCM controller for different implementations over $3T_f$. Table 3 summarizes the num-

Table 2: Number of Instructions in VCM Controller

Instructions	fast rate	slow rate	interlacing
Move	66	26	28
Mult/Add/Floating	45	15	20
Nop	45	15	10
Branch	0	3	5
Others	0	9	0

ber of computing cycles needed over $3T_f$ for fast rate PZT and different VCM controller

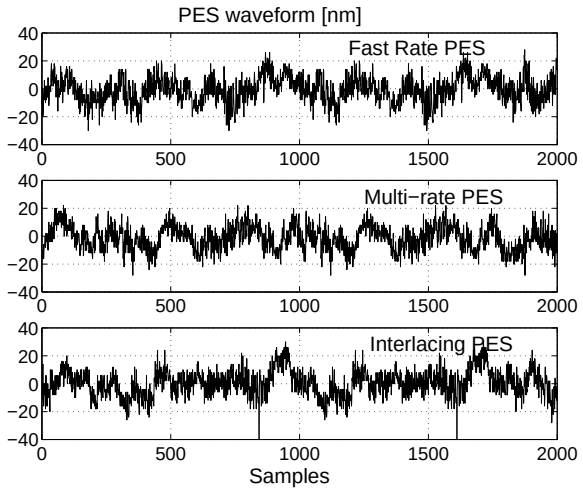

Figure 25: PES Waveform

implementation.

Table 3: Number of Instructions in VCM Controller

Scheme ($3T_f$)	fast rate PZT	fast rate VCM	slow rate VCM	interlacing VCM
cycles	159	123	57	53

Figure 25 shows the PES(position error signal) for PZT fast rate/VCM fast rate, PZT fast rate/VCM slow rate, and PZT fast rate/VCM interlacing . Notice that there are no significant differences among the three cases. Table 4 compares the three cases quantitatively in terms of 3σ(three times the standard deviation of PES) for each scheme.

Table 4: Number of Instructions in VCM Controller

Scheme	Fast rate	Multi-rate	interlacing
3σ	$26.0604nm$	$27.6706nm$	$27.6535nm$

From Tables 3 and 4, the multi-rate implementation without interlacing achieves about 36.3% computation saving with only about 6.2% performance degradation in terms of 3σ value and the multi-rate implementation with interlacing achieves about 38.5% computation saving with only about 6.1% performance degradation. This saving is significant since the

servo algorithm takes up more than 50% of the available DSP processing time in typical implementation[14].

6 Conclusion

In this report, multi-rate control is studied from the viewpoint of computation saving. The slow rate control algorithm may be decomposed and interlaced to make the amount of computation at fast sampling instances uniform. Lifting technique is used to analyze the multi-rate system. Practical performance indices are presented for evaluating disturbance rejection. Multi-rate control for computation saving is applied to a dual actuator disk file system. Dual actuator track following experiment verified that the proposed multi-rate scheme saves a significant amount of computation with little performance degradation. Various performance indices are computed and the proposed ones are shown to give realistic and less conservative measure of actual performance.

Acknowledgements

This research was conducted at the Computer Mechanics Laboratory(CML) in the Department of Mechanical Engineering, University of California at Berkeley. Mr. Yufeng Li's assistance in experiments is also acknowledged.

References

[1] D.T. Phan "The Design and Modeling of Multirate Digital Control System for Disk Drive Applications", *Proceedings of the 1993 Asia-Pacific Workshop on Advances in motion control*, Singapore, pp.189-205,July 1993.

[2] T. Hara and M. Tomizuka "Multi-rate Controller for Hard Disk Drive with Redesign of State Estimator", *Proceedings of the American Conference*, Philadephia, Pennsylvnia, June 1998.

[3] F.Marcassa and R.Oboe "Disturbance Rejection in Hard Disk Drives with Multi-rate Estimated State Feedback", *2nd IFAC Conference on Mechatronic Systems*,Berkeley, California, December, 2002

[4] J.Ding, C.Wu and M.Tomizuka " Settling Control with Reference Redesign for Dual Actuator Hard Disk Drive Systems", *2nd IFAC Conference on Mechatronic Systems*,Berkeley, California, December, 2002

[5] B.Bamieh, J.B.Pearson, and etc. "A lifting technique for linear periodic systems with applications to sampled-data control", *Systems & Control Letters*, vol.17, no.2, Aug. 1991, pp.79-88.

[6] Y.Gu and M.Tomizuka "Multirate digital redesign of continuous time controllers based on closed-loop performance" , Proceedings of the 2000 American Control Conference, vol.2, 2000, pp.1149-53 vol.2. Danvers, MA, USA.

[7] A.V. Oppenheim and R.W. Schafer, *Discrete-Time Signal Processing*, Prentice Hall, 2nd edition,1998.

[8] J.Ding, H.Numasato and M. Tomizuka "Single/dual-rate digital controller design for dual stage track folslowing in hard disk drives", *6th International Workshop on Advanced Motion Control*, Nagoya, Japan, pp80-85,April 2000.

[9] S.Wu and M. Tomizuka "Multirate Digital Control with Interlacing and Its Application to Hard Disk Drive Servo", submitted to 2003 American Control Conference.

[10] T.Chen and L.Qiu. "H_∞ design of general multirate sampled- data control systems",*Automatica* ,30 (7),1139-1152, 1994

[11] R.A.Meyer and C.S. Burrus, "A unified analysis of multirate and periodically time-varying digital filters," *IEEE Transactions on Automatic Control*, AC-35, pp423-443, 1990

[12] G.Strang and N.Truong *Wavelets and filter banks*,Wellesley, MA: Wellesley-Cambridge Press, c1996

[13] Grochowski and R. Hoyt, "Future trends in hard disk drives", *IEEE Transactions on Magnetics*, vol.32, pp.1850-1854, May 1996.

[14] H.Numasato, private communication

[15] K.Zhou , J. Doyle and K.Glover *Robust Optimal Control*, Prentice Hall, 1995